JCTC Journal of Chemical Theory and Computation

Article

Cite This: J. Chem. Theory Comput. 2019, 15, 2954−2965

pubs.acs.org/JCTC

Half-Projected σ Self-Consistent Field For Electronic Excited States

Hong-Zhou Ye and Troy Van Voorhis*

Department of Chemistry, Massachusetts Institute of Technology, Cambridge, Massachusetts 02139, United States

Supporting Information

ABSTRACT: Fully self-consistent mean-field solutions of electronic excited states have been much less accessible compared to ground state solutions (e.g., Hartree−Fock). The main reason for this is that most excited states are energy saddle points, and hence energy-based optimization methods such as Δ-SCF often collapse to the ground state. Recently, our research group has developed a new method, σ-SCF [*J. Chem. Phys.* 2017, *147*, 214104], that successfully solves the "variational collapse" problem of energy-based methods. Despite the success, σ-SCF solutions are often spin-contaminated for open-shell states due to the single-determinant nature; unphysical behaviors such as disappearing solutions and discontinuous first-order energy derivatives are also observed along with the spontaneous breaking of spin or spatial symmetries. In this work, we tackle these problems by partially restoring the broken spin-symmetry of a σ-SCF solution through an approximate spin-projection scheme called half-projection. Orbitals of the projected wave function are optimized in a variation-after-projection (VAP) manner. The resulting theory, which we term half-projected (HP) σ-SCF, brings substantial improvement to the description of singlet and triplet excitations of the original σ-SCF method. Numerical simulations on small molecules suggest that HP σ-SCF delivers high-quality excited-state solutions that exist in a wide range of geometries with smooth potential energy surfaces. We also show that local excitations in HP σ-SCF can be size-intensive.

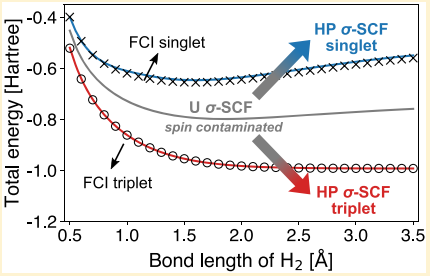

1. INTRODUCTION

The fast computation of mean-field excited states is important for two reasons. First, they provide a zeroth-order, qualitative description of the true, physical excited states; second, they can serve as a starting point for more accurate, correlated excited state methods.

Roughly speaking, existing methods for computing mean-field excited states can be divided into two classes. The first class consists of single-reference, linear response-based methods such as configuration interaction singles[1,2] (CIS) and time-dependent density functional theory[3−6] (TDDFT). These methods are able to compute single excitations from the reference state at a mean-field cost, with the computed excitation energies typically of electronvolt (eV) or even sub-eV accuracy for low-lying excitations.[7] However, methods from this class could fail in several ways. First, the dependence of the excited states on the reference state (usually the singlet ground state) makes these methods vulnerable when the reference is bad. Second, the effects of higher-order response are completely ignored in the linear-response treatment, which is responsible for the failure of these methods in situations where these effects are important.[8,9] Third, specifically for TDDFT, standard local or semilocal functionals perform poorly for Rydberg states and charge-transfer (CT) excitations due to the incorrect asymptotic behaviors of these functionals.[10−14] Many works have been reported to remedy some of these deficiencies. For instance, constricted variational-DFT[15−17] (CV-DFT), which can be viewed as perturbative extension of TDDFT within the Tamm−Dancoff approximation,[18] provides an approach to including the missing higher-order response and hence qualitatively correct descriptions of CT states even with local or semilocal approximate functionals.[8,9]

The second class of the mean-field excited state methods, on the other hand, treats both ground and excited states on an equal footing by directly seeking the excited states represented by the self-consistent solutions to either the Hartree−Fock (HF) or the Kohn−Sham (KS) equations. Perhaps the most well-known example of this class is Δ self-consistent field[19−21] (Δ-SCF), in which excited states are found by minimizing the energy of a nonaufbau electronic configuration. Despite the conceptual simplicity, the application of Δ-SCF is plagued by a severe numerical problem: the order of orbitals can change during the SCF iteration, which makes it difficult to converge to the desired states. This problem arises naturally from the fact that excited states are often energy saddle points and hence difficult to locate in general. For this reason, several methods such as the maximum overlap method[22] (MOM) or SCF metadynamics[23] have been introduced and demonstrated some success. However, strong dependence on a good initial guess still mandates expertise. Nevertheless, when these methods do converge to the desired states, the quality of the solutions is often similar or even superior to the methods from the previous class, especially for hard cases such as CT states.[22] More importantly, the resulting excited states, being not orthogonal to each other, can be used as quasi-diabatic bases in correlated methods such as nonorthogonal configuration interaction (NOCI).[24−26]

Received: December 6, 2018
Published: April 17, 2019

DOI: 10.1021/acs.jctc.8b01224
J. Chem. Theory Comput. 2019, 15, 2954−2965

Recently, our research group and others have extended the use of ground-state variational principle for excited states.[27−30] In these methods, some quantities other than energy are subject to variational optimization; these quantities possess the ideal property that both ground and excited states are local *minima* in Hilbert space, rendering the optimization of them numerically stable. The minimum corresponding to the desired excited state is often targeted by performing a direct energy-targeting[31] (DET) calculation prior to the variational optimization. This general scheme of computing excited states has been explored at both mean-field[28,30] and correlated levels.[27] In this work, we focus on a specific method from this class, σ-SCF,[28] in which the *energy variance* of a single Slater determinant is variationally optimized. Equipped with DET, σ-SCF is found to be very effective at locating excited states, including individual, high energy excitations within a dense manifold of excited states; the quality of σ-SCF solutions is similar to that of the energy-based, self-consistent mean-field solutions obtained from Δ-SCF, enabling further improvements via electron correlation methods.[28]

Despite the success, several problems have been reported for σ-SCF. First, the well-known symmetry breaking problem—which has been investigated extensively for mean-field ground states[32−36]—is also present in the σ-SCF solutions of mean-field excited states. Specifically, the ubiquitous open-shell configurations in excited states lead to the spontaneous breaking of spin symmetry (a phenomenon known as spin-contamination), which deteriorates the energy and other properties computed from the σ-SCF wave function.[28] Second, empirical observations suggest that the energy of a σ-SCF solution, while being a continuous function of the molecular geometry, could show discontinuity in its first-order derivatives (i.e., atomic forces) at symmetry-breaking points. Moreover, some spurious solutions that do not correspond to any physical states have been found by σ-SCF, while some other solutions that are of physical significance disappear beyond certain geometries.[28] These problems altogether hinder further applications of σ-SCF to more complicated systems.

As suggested by many seminal works on ground-state mean-field theories, symmetry breaking-related problems could be solved by restoring the broken symmetries through projection of the wave function onto the eigenstate of the corresponding symmetry operators.[37−39] This idea, called symmetry-projection, was first introduced by Löwdin in the 1950s in his extended Hartree−Fock[40] (EHF) theory (also known as projected Hartree−Fock or PHF) and later on pursued by many others[41−45] (see ref 37 for a comprehensive review). However, even for systems of moderate size, the optimization of a fully projected wave function leads to nonlinear, self-consistent equations that are extremely complicated to solve.[37] For this reason, further development of PHF ceased in the 1980s. It was only recently that the seemingly formidable variation-after-projection (VAP) problem has been solved by Scuseria et al. in the projected quasi-particle theory[38] (PQT), which is capable of handling the breaking and restoration of many symmetries within the same framework at only a mean-field computational cost. PQT and its variants[39] are found to be effective at recovering the static part of electron correlation that arises from symmetry breaking.[46−49] Extensions of PQT to DFT[50,51] and quantum Monte Carlo[52] (QMC) have also been reported to include dynamic correlation.

Despite this recent development of PHF, performing the exact symmetry-projection still requires SCF programs that are algorithmically complicated. If spin is the only relevant symmetry subject to restoration (as in σ-SCF), many approximate strategies have been proposed to avoid the cost of performing a full spin-projection.[53−63] In this work, we are particularly interested in one such approximation, called half-projected HF (HPHF), which was developed by Smeyers et al.[58,59] and by Cox and Wood[62,63] in the 1970s. In HPHF, the energy is minimized variationally for a special two-determinant wave function (eq 3), which can be regarded as a spin-unrestricted HF (UHF) wave function projected onto the subspace of even or odd spin quantum numbers and hence can be used to approximate the exact singlet and triplet states, respectively. For singlet ground states of small molecules, HPHF has been shown to generate results that are comparable to those from PHF, at merely twice the computational cost of a UHF calculation.[58−63]

In this work, we apply the half-projection scheme to σ-SCF in order to reduce the spin-contamination and hence mitigate the spin symmetry-breaking-related problems in σ-SCF excited states. The resulting theory, termed HP σ-SCF, exhibits improvement over the original σ-SCF method in two ways. First, HP σ-SCF recovers part of the static correlation by adopting a special two-determinant wave function and delivers potential energy surfaces (PESs) that reproduce the qualitative shape of the exact solutions in cases where the major source of spin-contamination is the mix of singlet and triplet states. Second and perhaps more importantly, solutions found by HP σ-SCF are more physical compared to those from the unprojected theory, in the sense that they correspond to PESs that show less derivative discontinuities and exist in a wider range of geometries, which are key to the application of electron correlation methods such as NOCI.

This paper is organized as follows. In section 2, we present a detailed, formal discussion on the theory of HP σ-SCF. In section 3, we present the computational details. In section 4, we present numerical results of three representative molecules along with some discussion. In section 5, we conclude this work by pointing out several future directions.

2. THEORY

In this section, we present formal discussion of HP σ-SCF. Throughout this paper, we adopt the notations where μ, ν, ... index one-electron basis functions [e.g., atomic orbitals (AOs)]; i, j, ... and a, b, ... index occupied and virtual molecular orbitals (MOs); p and q index unspecified MOs; s and t index the z component of electron spin. Real-valued orbitals are assumed.

2.1. HP Wave Function. Consider a spin-unrestricted Slater determinant

$$|\Phi\rangle = |\phi_1^{\alpha}\overline{\phi}_1^{\beta}\cdots\phi_N^{\alpha}\overline{\phi}_N^{\beta}\rangle \tag{1}$$

where $\{\phi_i^{\alpha}\}_{i=1}^N$ and $\{\phi_i^{\beta}\}_{i=1}^N$ are two sets of one-electron orbitals (the overline denotes spin β). Although spin-compensated, $|\Phi\rangle$ is in general not a pure singlet due to the so-called spin-contamination from higher-spin components[64]

$$|\Phi\rangle = c_S|S\rangle + c_T|T\rangle + c_Q|Q\rangle + \cdots \tag{2}$$

where S, T, Q, and etc. are singlet, triplet, quintet, and so on. Ideally, all components of unwanted spin can be removed by projecting $|\Phi\rangle$ onto the subspace of the desired spin quantum number, which is exactly what PHF and PQT do.[38,40] The half-

DOI: 10.1021/acs.jctc.8b01224
J. Chem. Theory Comput. 2019, 15, 2954−2965

projection method approximates this process with the following HP wave function[58,62]

$$|\Psi_\eta\rangle = \frac{1}{\sqrt{2}}(|\Phi\rangle + \eta|\bar{\Phi}\rangle), \quad \eta = \pm 1 \tag{3}$$

where $|\bar{\Phi}\rangle = |\phi_1^\beta \bar{\phi}_1^\alpha \cdots \phi_N^\beta \bar{\phi}_N^\alpha\rangle$ is the spin conjugate of $|\Phi\rangle$. Since

$$|\bar{\Phi}\rangle = c_S|S\rangle - c_T|T\rangle + c_Q|Q\rangle - \cdots \tag{4}$$

the linear combination in eq 3 removes the contamination from states of odd or even spin for $\eta = +1$ or -1, respectively. As a result, $|\Psi_+\rangle$ is a good approximation to the exact singlet due to the removal of triplet, which is usually the largest component in the contamination of a singlet state. Similar arguments suggest that $|\Psi_-\rangle$ is a good approximation to the exact triplet. Note that eq 3 can also be viewed as a two-point approximation (with equal weight) to the exact spin-projection used in spin-projected unrestricted Hartree−Fock[46,48,65] (SUHF).

In general, the HP wave function defined in eq 3 is not normalized (the coefficient $\frac{1}{\sqrt{2}}$ is merely a convention rather than a normalization constant)

$$\langle\Psi_\eta|\Psi_\eta\rangle = 1 + \eta D \tag{5}$$

where $D = \langle\Phi|\bar{\Phi}\rangle$ is the overlap matrix element between Φ and its spin conjugate. As will be clear in section 2.5, $D \in [0, 1]$, where $D = 1$ corresponds to the spin-restricted case (i.e., $\phi_i^\alpha = \phi_i^\beta$ for all i's).

With these definitions, the energy of a HP wave function can be written as

$$E_\eta = \frac{\langle\Psi_\eta|\hat{H}|\Psi_\eta\rangle}{\langle\Psi_\eta|\Psi_\eta\rangle} = \frac{E_1 + \eta D E_2}{1 + \eta D} \tag{6}$$

where $\hat{H}$ is the electronic Hamiltonian [eq 10], and

$$E_1 = \langle\Phi|\hat{H}|\Phi\rangle, \quad E_2 = \frac{\langle\Phi|\hat{H}|\bar{\Phi}\rangle}{\langle\Phi|\bar{\Phi}\rangle} \tag{7}$$

are the UHF energy and the (normalized) cross energy, respectively. Similarly, the energy variance of a HP wave function takes the following form

$$\sigma_\eta^2 = \frac{\langle\Psi_\eta|(\hat{H} - E_\eta)^2|\Psi_\eta\rangle}{\langle\Psi_\eta|\Psi_\eta\rangle} = \frac{\sigma_1^2 + \eta D\sigma_2^2 + \frac{\eta D}{1+\eta D}(E_1 - E_2)^2}{1 + \eta D} \tag{8}$$

where

$$\sigma_1^2 = \langle\Phi|(\hat{H} - E_1)^2|\Phi\rangle, \quad \sigma_2^2 = \frac{\langle\Phi|(\hat{H} - E_2)^2|\bar{\Phi}\rangle}{\langle\Phi|\bar{\Phi}\rangle} \tag{9}$$

are the UHF energy variance and (normalized) cross energy variance, respectively. Detailed expressions of these integrals will be given in the next section.

2.2. Energy and Energy Variance of an HP Wave Function. In this section, we derive expressions for the energy and the energy variance of an HP wave function as defined in eqs 6 and 8; the optimization of the energy variance, which is the key to HP σ-SCF, will be discussed in the subsequent section.

Consider the following Hamiltonian

$$\hat{H} = \sum_s \sum_{\mu\nu}^K h_{\mu\nu} c_{\mu s}^\dagger c_{\nu s} + \frac{1}{2}\sum_{st}\sum_{\mu\nu\lambda\sigma}^K (\mu\nu|\lambda\sigma) c_{\mu s}^\dagger c_{\lambda t}^\dagger c_{\sigma t} c_{\nu s} \tag{10}$$

where $h_{\mu\nu}$ and $(\mu\nu|\lambda\sigma)$ are one- and two-electron integrals [in the (11|22) notation] in a set of K orthonormal basis functions, $\{\chi_\mu\}$, which are created and annihilated by $\{c_{\mu s}^\dagger\}$ and $\{c_{\mu s}\}$, respectively. In terms of these basis functions, orbitals in the HP wave function $|\Psi_\eta\rangle$ can be represented by column vectors in the coefficient matrices (the first N columns being occupied), $\{\boldsymbol{C}^s\}$, such that

$$\phi_p^s = \sum_\mu^K C_{\mu p}^s \chi_\mu \tag{11}$$

Note that for basis functions we have $\chi_\mu^\alpha = \chi_\mu^\beta \equiv \chi_\mu$. The overlap integral between Φ and $\bar{\Phi}$, as defined in eq 5, is then given by

$$D = \det \boldsymbol{S}^{\alpha\beta} \det \boldsymbol{S}^{\beta\alpha} = |\det \boldsymbol{S}^{\alpha\beta}|^2 \tag{12}$$

where

$$S_{ij}^{\alpha\beta} = \sum_\mu^K C_{\mu i}^\alpha C_{\mu j}^\beta \tag{13}$$

is the overlap matrix between α and β orbitals.

In order to obtain concise expressions for energy and energy variance, we define the density matrices

$$P_{\mu\nu}^s = \langle\Phi|c_{\nu s}^\dagger c_{\mu s}|\Phi\rangle = \sum_i^N C_{\mu i}^s C_{\nu i}^s \tag{14}$$

and the (normalized) cross density matrices

$$P_{\mu\nu}^{s\bar{s}} = \frac{\langle\Phi|c_{\nu s}^\dagger c_{\mu s}|\bar{\Phi}\rangle}{\langle\Phi|\bar{\Phi}\rangle} = \sum_{ij}^N C_{\mu i}^{\bar{s}} M_{ij}^{s\bar{s}} C_{\nu j}^s \tag{15}$$

where $\boldsymbol{M}^{s\bar{s}} = (\boldsymbol{S}^{s\bar{s}})^{-1}$ is the inverse matrix of the overlap matrix defined in eq 13. Note that eq 15 is valid only when D is nonzero; the generalization to handle some $D = 0$ cases can be found in ref 62. We further define the Fock matrices

$$F_{\mu\nu}^s = h_{\mu\nu} + \sum_{\lambda\sigma}^K (\mu\nu|\lambda\sigma) P_{\sigma\lambda} - (\mu\sigma|\lambda\nu) P_{\sigma\lambda}^s \tag{16}$$

and the (normalized) cross Fock matrices

$$F_{\mu\nu}^{s\bar{s}} = h_{\mu\nu} + \sum_{\lambda\sigma}^K (\mu\nu|\lambda\sigma) \bar{P}_{\sigma\lambda} - (\mu\sigma|\lambda\nu) P_{\sigma\lambda}^{s\bar{s}} \tag{17}$$

where $\boldsymbol{P} = \sum_s \boldsymbol{P}^s$ and $\bar{\boldsymbol{P}} = \sum_s \boldsymbol{P}^{s\bar{s}}$ are the total density matrix and the total (normalized) cross density matrix, respectively.

In terms of these quantities, the matrix elements required for computing the HP energy [eq 6] and energy variance [eq 8] can be derived using the generalized Wick's theorem.[66,67] The results are

$$E_1 = \frac{1}{2}\mathrm{Tr}\left(\boldsymbol{h}\boldsymbol{P} + \sum_s \boldsymbol{F}^s \boldsymbol{P}^s\right) \tag{18}$$

$$E_2 = \frac{1}{2}\mathrm{Tr}\left(\boldsymbol{h}\bar{\boldsymbol{P}} + \sum_s \boldsymbol{F}^{s\bar{s}} \boldsymbol{P}^{\bar{s}s}\right) \tag{19}$$

DOI: 10.1021/acs.jctc.8b01224
J. Chem. Theory Comput. 2019, 15, 2954−2965

$$\sigma_1^2 = \sum_s \Bigg\{ \mathrm{Tr}\boldsymbol{P}^s\boldsymbol{F}^s\boldsymbol{Q}^s\boldsymbol{F}^s + \frac{1}{2}P^s_{\mu\mu'}Q^s_{\nu\nu'}P^s_{\lambda\lambda'}Q^s_{\sigma\sigma'} \times (\mu\nu|\lambda\sigma)[(\mu'\nu'|\lambda'\sigma') - (\mu'\sigma'|\lambda'\nu')] + \frac{1}{2}P^s_{\mu\mu'}Q^s_{\nu\nu'}P^{\bar{s}}_{\lambda\lambda'}Q^{\bar{s}}_{\sigma\sigma'}(\mu\nu|\lambda\sigma)(\mu'\nu'|\lambda'\sigma') \Bigg\} \tag{20}$$

$$\sigma_2^2 = \sum_s \Bigg\{ \mathrm{Tr}\boldsymbol{P}^{s\bar{s}}\boldsymbol{F}^{\bar{s}s}\boldsymbol{Q}^{s\bar{s}}\boldsymbol{F}^{\bar{s}s} + \frac{1}{2}P^{s\bar{s}}_{\mu\mu'}Q^{\bar{s}s}_{\nu\nu'}P^{s\bar{s}}_{\lambda\lambda'}Q^{\bar{s}s}_{\sigma\sigma'} \times (\mu\nu|\lambda\sigma)[(\mu'\nu'|\lambda'\sigma') - (\mu'\sigma'|\lambda'\nu')] + \frac{1}{2}P^{s\bar{s}}_{\mu\mu'}Q^{\bar{s}s}_{\nu\nu'}P^{\bar{s}s}_{\lambda\lambda'}Q^{s\bar{s}}_{\sigma\sigma'}(\mu\nu|\lambda\sigma)(\mu'\nu'|\lambda'\sigma') \Bigg\} \tag{21}$$

where $\boldsymbol{Q}^s = \boldsymbol{I} - \boldsymbol{P}^s$, $\boldsymbol{Q}^{\bar{s}} = \boldsymbol{I} - \boldsymbol{P}^{\bar{s}}$, and Einstein summation rule is assumed for AO indices. We have checked the correctness of these formulas using a homemade full CI code.

2.3. Optimization of the HP Wave Function. In HP σ-SCF, we perform full orbital optimization for the HP wave function in a self-consistent variation-after-projection (VAP) manner. This scheme is known to be more general than the projection-after-variation (PAV) approach.[38,39,68] Specifically, the HP wave function is subject to the following variance minimization

$$|\Psi^*_\eta\rangle = \arg\min_{\Psi_\eta} \sigma^2_\eta \tag{22}$$

which is analogous to HPHF that minimizes the HP energy. A Fock matrix can be derived by directly differentiating σ^2_η with respect to the idempotent density matrix (eq 14). The result is

$$\mathcal{F}^s_\eta = (\mathcal{F}^s_\eta)_1 + \eta D[(\mathcal{F}^s_\eta)_2 + (\mathcal{F}^s_\eta)^\dagger_2] \tag{23}$$

where we guide the readers to the Supporting Information for detailed expressions of $(\mathcal{F}^s_\eta)_1$ and $(\mathcal{F}^s_\eta)_2$ (section S1). One can show that the HP σ-SCF Fock matrices given in eq 23 satisfy the generalized Brillouin theorem,[69−72] i.e.

$$\langle\phi^s_i|\mathcal{F}^s_\eta|\phi^s_a\rangle = 0 \tag{24}$$

and hence are compatible with the Cox and Wood approach of deriving the HPHF Fock matrices,[62] where ϕ^s_i and ϕ^s_a are arbitrary occupied and virtual orbitals of spin s.

With the HP σ-SCF Fock matrix in hand, one can solve the following Roothaan-like equations

$$\mathcal{F}^s_\eta\boldsymbol{C}^s = \boldsymbol{C}^s\mathcal{L}^s \tag{25}$$

using the standard SCF procedure to obtain the optimum HP σ-SCF orbitals, where $\mathcal{L}^s = \mathrm{diag}\{l^s_1, l^s_2, \cdots, l^s_K\}$ are the HP σ-SCF orbital variances. Numerically, we have verified that eq 25 gives the correct HP σ-SCF states by comparing them to the solutions of direct minimization of the HP variance. We further note that, at convergence, the idempotent density matrices commute with the HP σ-SCF Fock matrices; thus, extrapolation algorithms such as Pulay's direct inversion of iterative space[73] (DIIS) can be used to accelerate the SCF process.

2.4. Targeting a Specific State. The variance optimization discussed above transforms the eigenspectrum of the electronic Hamiltonian into a set of (local) minima on the energy variance landscape; the remaining task is to target the specific minimum corresponding to the desired excited state. To that end, we first optimize the following direct energy-targeting (DET) functional[27,28,74]

$$W[\Psi_\eta](\omega) = \frac{\langle\Psi_\eta|(\hat{H} - \omega)^2|\Psi_\eta\rangle}{\langle\Psi_\eta|\Psi_\eta\rangle} \tag{26}$$

and then refine its solution by a variance minimization. The net result of this two-step algorithm is the HP σ-SCF state whose energy is *closest* to ω. In other words, the single parameter ω serves as the energy target for any excitation. Furthermore, with a simple bracketing algorithm,[75] one could in principle compute all excited states in a given energy window.

In practice, the minimization of $W[\Psi_\eta](\omega)$ can also be turned into a set of Roothaan-like equations resembling eq 25. The corresponding Fock matrices can be derived in a similar approach as in section 2.3; the results can be found in the Supporting Information (section S2). Like the variance minimization, the DET Fock matrices commute with the density matrices at convergence, which enables DIIS to accelerate the SCF convergence.

2.5. Some Properties. Before presenting numerical results, we briefly summarize some properties of HP σ-SCF.

First, as a variance-based variational method, HP σ-SCF is distinct from energy-based methods in several aspects. (i) The HP energy does not obey the Hellmann−Feynman theorem,[76,77] which means that the evaluation of energy derivatives, such as atomic forces, requires the computationally expensive derivative of the wave function. (ii) The HP σ-SCF solutions are quasi-diabatic and do not show avoided crossing; these features render HP σ-SCF a complementary method to the deductive strategies of constructing approximate diabatic states, such as methods that enforce configurational uniformity.[78,79] (iii) As mentioned in section 1 and shown in ref 28, the first-order energy derivative of an unprojected σ-SCF solution may be discontinuous when it undergoes symmetry breaking. In principle, this problem could occur for HP σ-SCF states, too, due to both the inexact spin-projection and the breaking of symmetries other than spin. However, as we will see in section 4, all HP σ-SCF solutions found in this work deliver smooth potential energy surfaces, evidently due to the effect of the spin-projection.

Second, as other HP methods, HP σ-SCF improves upon the original σ-SCF in two ways: reducing the spin-contamination and recovering some static correlation energy. The detailed, formal discussion can be found in Supporting Information (section S3). Here, we only emphasize one limit of HP methods. Due to the special form of the HP wave function (eq 3), the number of (partially) occupied natural orbitals (NOs) is limited by the number of electrons in the system. Thus, the HP wave function cannot provide a qualitative description of the electronic structure if a large number of NOs are occupied in the exact solution. Nevertheless, we will see in section 4 that these strongly correlated states can be described by invoking a NOCI calculation based on the HP σ-SCF solutions.

2.6. Computational Scaling. We end this section by commenting on the computational cost of HP σ-SCF. Like other mean-field SCF methods, the computational bottleneck is building the HP σ-SCF Fock matrix, which is approximately twice the cost of forming the unprojected σ-SCF Fock matrix. Hence, we conclude that the overall computational scaling of HP σ-SCF is the same as that of σ-SCF, which is formally

DOI: 10.1021/acs.jctc.8b01224
J. Chem. Theory Comput. 2019, 15, 2954−2965

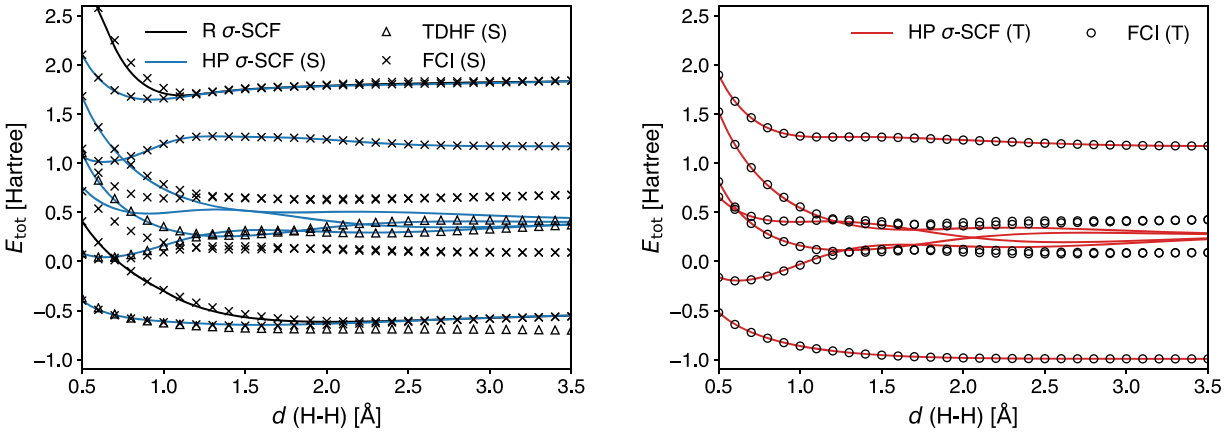

Figure 1. Comparison of HP σ-SCF, TDHF (with RHF reference), and FCI potential energy surfaces of 3-21G H_2 (left singlet; right triplet). Two R σ-SCF solutions that are stable to spin-projection are also included.

$O(K^5)$ in time and $O(K^2)$ in memory according to our previous work.[28] We also note that this scaling mirrors that of the Laplace transform Møller−Plesset perturbation theory of second order[80] (MP2), which is a result of the formal similarity between the expressions of the mean-field energy variance and the MP2 correlation energy. Thus, one can expect a better scaling for systems of large size where sparsity comes into play.

3. COMPUTATIONAL DETAILS

In the following computational work, atom-centered, Gaussian-type orbitals (i.e., atomic orbitals or AOs) are used as the basis functions, with necessary AO integrals computed in `Psi4`.[81] Molecular geometries are optimized at the CCSD(T)/cc-pVTZ[82] level as implemented in Q-Chem.[83] Both HP σ-SCF and the original σ-SCF calculations are performed in `frankenstein`.[84] All calculations presented below are performed using small AO bases due to our preliminary implementation. To target a specific HP σ-SCF state, we either perform a DET calculation as described in section 2.4 prior to the HP variance optimization or simply use the corresponding σ-SCF solution as an initial guess. When the latter is used, the starting wave function might be spin-restricted (i.e., R σ-SCF); in that case, one can manually break the spin symmetry by perturbing either the α or the β orbitals through, e.g., mixing the occupied and the virtual orbitals. We note the reader that this does not always lead to a HP state, since it is possible that the R σ-SCF solution we initially have is stable to half-projection in the sense that its energy variance is lower than any HP σ-SCF solutions lying close to it on the energy variance landscape. To follow a PES, the optimized orbitals from the adjacent geometry are used as initial guess for the calculation of current geometry. DIIS is always turned on to accelerate the SCF convergence. For all molecules investigated in this work, the exact solutions are available for comparison through either a homemade FCI or density matrix renormalization group[85,86] (DMRG) as implemented in `Block`.[87−91] In addition to the exact solutions, we also compare HP σ-SCF to other excited state methods, including time-dependent Hartree−Fock[92] (TDHF) as implemented in PySCF[93] and state-averaged complete active space self-consistent field[94] (SA-CASSCF) as implemented in Gaussian 03.[95]

4. RESULTS AND DISCUSSION

4.1. 3-21G H_2. The first molecule we consider is H_2 in a double-ζ basis set, 3-21G.[96] Since H_2 is a two-electron system, the only spin contamination arises from mixing triplet states into singlet states, which makes the half-projection equivalent to the full spin-projection in this special case. Thus, H_2 serves as an ideal system to investigate the effect of spin-projection on broken-symmetry mean-field excited states. The results comparing HP σ-SCF and FCI are presented in Figure 1 for both singlet and triplet states. TDHF solutions based on a RHF reference are also included for singlet. The results of the corresponding unprojected σ-SCF method can be found in the Supporting Information (Figure S1).

Several observations can be made from Figure 1. First, spin-projection leads to high accuracy for both singlet and triplet spins and for most states and bond lengths, which is a significant improvement upon the unprojected σ-SCF solutions (Figure S1 in the Supporting Information). The only regime where HP σ-SCF fails to follow the FCI solutions is the states of intermediate energy (0−1 hartree) at stretched geometries: four HP σ-SCF solutions wiggle in between the exact curves, cross each other, and show incorrect asymptotic behaviors at the dissociation limit. Analysis of the NOs suggests that these FCI solutions are truly multiconfigurational, with all NOs (four in this case) displaying fractional occupation. The accurate description of these states is beyond the capability of HP σ-SCF, which has only one pair of NOs being fractionally occupied (due to H_2 being a two-electron system) according to our discussion in section 2.5. Nevertheless, this multireference character can be well captured by invoking a nonorthogonal configuration interaction (NOCI) calculation based on the relevant HP σ-SCF states; we guide the readers to the Supporting Information for such a treatment (Figure S2).

Second, HP σ-SCF shows a favorable comparison with TDHF, as the latter only finds three singly excited states due to its linear response nature. Notably, the two TDHF states in the strongly correlated regime as discussed above coalesce with two of the HP σ-SCF states. Unlike HP σ-SCF, however, the TDHF solutions cannot be further improved by NOCI since the underlying objects in TDHF are response vectors rather than wave functions.

Last but not least, all the unphysical behaviors associated with the unprojected σ-SCF solutions are removed by the spin-projection: the PESs shown in Figure 1 exist and are smooth

DOI: 10.1021/acs.jctc.8b01224
J. Chem. Theory Comput. 2019, 15, 2954−2965

for all geometries investigated here, which is crucial to the NOCI treatment discussed above. A specific example is displayed in Figure 2, where one can see that the unprojected

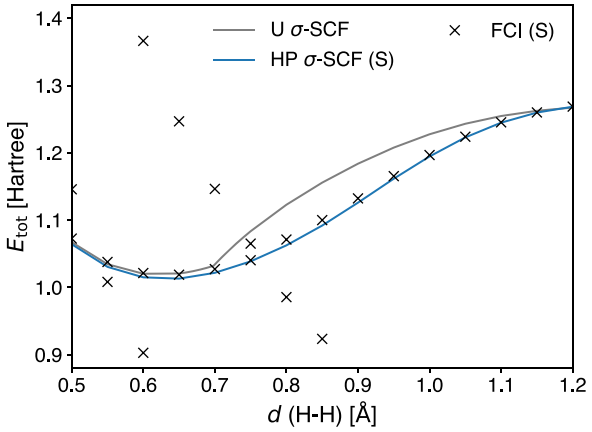

Figure 2. Zoom-in view of the symmetry-breaking point of a selected U σ-SCF solution (gray) and the corresponding singlet HP σ-SCF curve (blue) of 3-21G H_2. Relevant FCI states (black cross) are also included. The U σ-SCF solution breaks both the spin and mirror symmetry at d(H−H) ≈ 0.7 Å, while the HP solution restores the spin symmetry but extends the breaking of the spatial symmetry to d(H−H) < 0.7 Å, too.

U σ-SCF PES is kinked at d(H−H) ≈ 0.7 Å, while the HP σ-SCF solution smoothly transitions among several FCI states. An inspection of the optimized orbitals suggests that the U σ-SCF solution also breaks the spatial (i.e., mirror) symmetry at the kink; this symmetry breaking is not restored by the spin projection but instead stabilized: the HP σ-SCF solution breaks the mirror symmetry for all bond lengths investigated here. Thus, in this specific case, the smoothness of the HP σ-SCF solution is not a consequence of restoring all broken symmetries, but an outcome of restoring one (spin) while changing the regime of stability of the other (spatial).

4.2. 3-21G LiH. The second example we choose is LiH in a double-ζ basis set, 3-21G.[96] Since LiH has four electrons, the half-projection is still exact for triplet but merely an approximation for singlet due to the spin-contamination from quintets. Smeyers has shown that for the singlet ground state of LiH, HPHF is still as good as EHF,[97] potentially due to the relatively high energy of quintets, which consequently do not mix strongly with the ground state. For the same reason, one could expect half-projection to be an effective approximation to the first several, low-lying excitations of LiH, too. The results comparing HP σ-SCF and FCI for these states are presented in Figure 3 for both singlet and triplet. TDHF solutions based on a RHF reference are also included for singlet. The results of the corresponding unprojected σ-SCF method can be found in the Supporting Information (Figure S3).

From Figure 3, one can see that HP σ-SCF solutions, as expected, demonstrate high accuracy for both singlet and triplet spins. HP σ-SCF also compares favorably with TDHF, which misses the highest-energy excitation in Figure 3 (which is a doubly excited state according to population analysis) and predicts incorrect asymptotic behaviors for all other states due to the RHF reference behaving qualitatively wrong in that regime. Moreover, the HP σ-SCF solutions are quasi-diabatic and smoothly transition in between different FCI states in the region where they show avoided crossing. We also note that the state disappearing problem is mitigated significantly compared to the U σ-SCF solutions (Figure S3), especially for the triplet spin where half-projection is exact.

4.3. STO-3G C_2H_4. The third example is the C−C bond rotation of C_2H_4 in its minimal basis, STO-3G.[98] Unlike the previous two examples, the half-projection is a much cruder approximation to the full spin-projection due to the increasing number of electrons. Hence, it is of significant importance to investigate how HP σ-SCF performs in this case. The results for the first ten singlet and triplet states are presented in Figure 4, with all HP σ-SCF solutions having been shifted downward by 0.124 53 hartree to match the DMRG singlet ground state at zero torsion (i.e., $\theta = 0°$). The SA-CASSCF solutions using an active space of four orbitals and four electrons and averaged over the first eight singlet states with equal weight are also included in a separate figure for comparison (Figure 5); these solutions are shifted downward by 0.117 21 hartree for the same reason as above. The unprojected σ-SCF results can be found in the Supporting Information (Figure S4).

Several observations can be made from Figure 4 and 5. First, HP σ-SCF provides a good description to both singlet and triplet ground states, even in the regime of maximal torsion (i.e., $\theta = 90°$); the singlet HP σ-SCF ground state also shows similar accuracy compared to SA-CASSCF(4,4). These

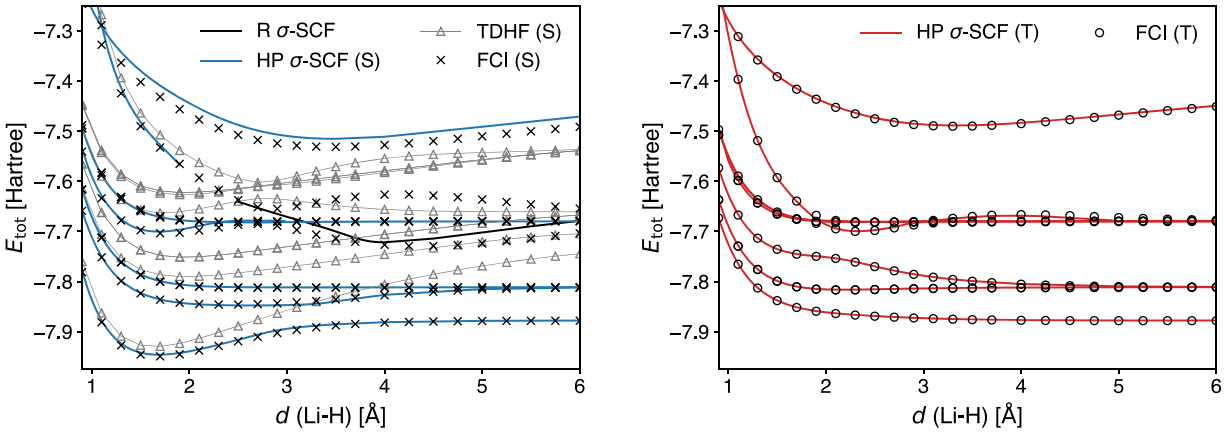

Figure 3. Comparison of HP σ-SCF, TDHF (with RHF reference), and FCI potential energy surfaces of 3-21G LiH dissociation (left singlet; right triplet). The RHF solution is included as the lowest TDHF state. One R σ-SCF solution that is stable to half-projection is also included.

DOI: 10.1021/acs.jctc.8b01224
J. Chem. Theory Comput. 2019, 15, 2954−2965

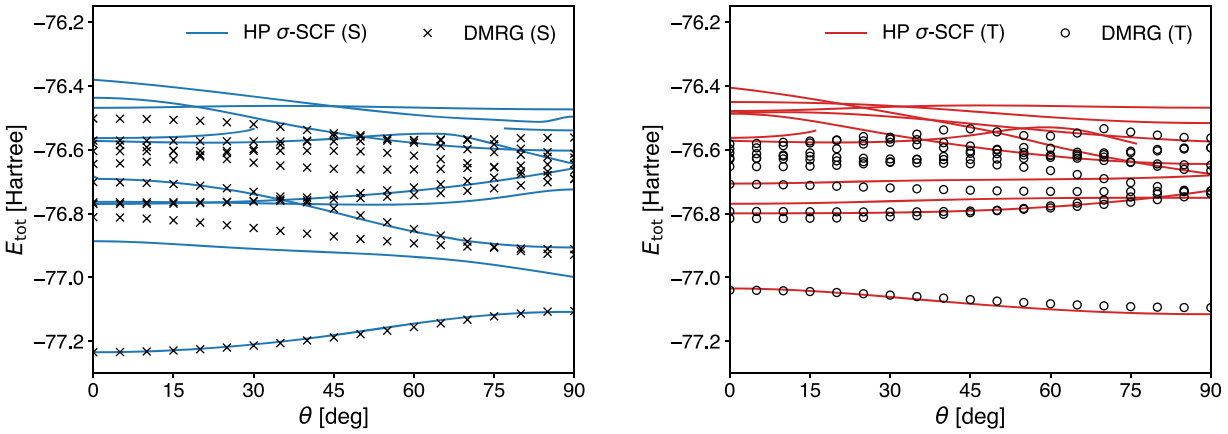

Figure 4. Comparison of HP σ-SCF and DMRG potential energy surfaces of the C−C bond rotation of C_2H_4 in STO-3G (left singlet; right triplet). All HP σ-SCF solutions have been shifted downward by 0.124 53 hartree to match the DMRG singlet ground state at $\theta = 0°$.

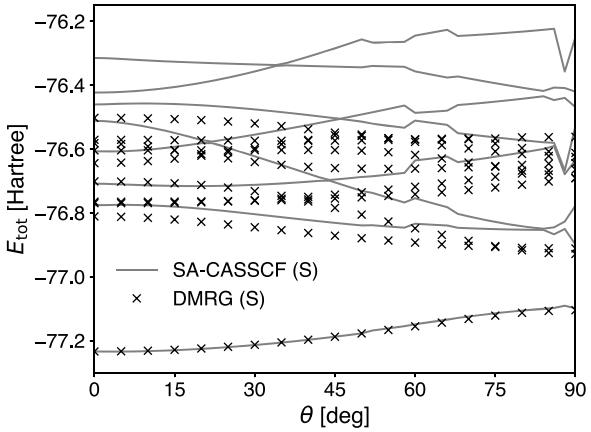

Figure 5. Comparison of SA-CASSCF(4,4) and DMRG singlet potential energy surfaces of the C−C bond rotation of C_2H_4 in STO-3G. The orbitals of the CAS calculation are optimized by averaging the first eight singlet states with equal weight; the bumps on the energy curves are potentially due to state-flipping. All SA-CASSCF solutions have been shifted downward by 0.117 21 hartree to match the DMRG singlet ground state at $\theta = 0°$.

observations highlight a significant improvement over the unprojected σ-SCF solutions (Figure S4 in the Supporting Information) and indicate the recovering of static correlation. Second, HP σ-SCF manages to capture the qualitative feature of the dense excited state spectrum of DMRG, such that an approximate one-to-one mapping can be identified between most HP σ-SCF and DMRG solutions. However, quantitative predictability is limited due to the spin-contamination from low-energy quintets (for HP singlets) and septets (for HP triplets) that is not removed at the half-projection level, as well as the electron correlation not captured by the two-determinant HP wave function. Nevertheless, HP σ-SCF still compares favorably with SA-CASSCF(4,4), which predicts excitation energy that is too high for the regime of small torsion and gives discontinuous energy curves for large torsion angles (potentially due to state-flipping[99]). Population analysis suggests that all the singlet HP σ-SCF states presented here correspond to excitations mainly within the (4,4) active space. Hence, this comparison highlights the effect of both spin-projection and state-specific orbital optimization for excited states. Last but not least, state disappearing of HP σ-SCF is more common than previous examples due to the stronger spin-contamination. In summary, these observations reveal the need for methods that can capture *more* electron correlation and perform more accurate spin-projection in large molecules.

4.4. Noninteracting He Atoms. In the last example, we investigate the size-extensivity of HP σ-SCF excitation energy. It is well-known that PHF is neither size-extensive nor size-consistent;[100−103] hence, the correction of spin-projection on extensive quantities such as atomization energy will vanish in the thermodynamic limit.[39] However, since excitation energy is a size-intensive quantity, spin-projection could potentially have nonzero effect even in the thermodynamic limit.

To that end, we consider five types of local excitations of noninteracting He atoms (Figure 6) using the 6-31G basis[104]

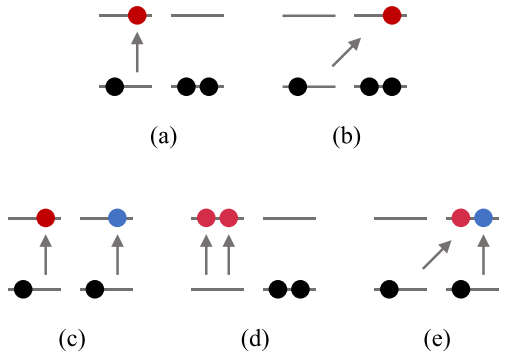

Figure 6. Five types of local excitations of noninteraction He atoms: (a) local single, (b) charge transfer, (c) simultaneous local singles, (d) local double, and (e) local single and charge transfer.

that have been investigated by Tsuchimochi and Van Voorhis using time-dependent spin-projected unrestricted Hartree−Fock[68] (TDSUHF). In their study, the single excitation energies (a and b) of TDSUHF converge asymptotically to the unprojected TDHF values in the thermodynamic limit, while the double excitation energies (c, d, and e) converge to some nonzero constants different from the triplet TDHF energies.[68] Our results of HP σ-SCF are shown in Table 1.

Unlike TDSUHF, the HP σ-SCF excitation energies are size-intensive for all types of excitations in Figure 6 except for d. An inspection of the optimized orbitals suggests that the excited state HP σ-SCF wave functions of n He atoms can be factorized into a direct product of a HP σ-SCF excited state

DOI: 10.1021/acs.jctc.8b01224
J. Chem. Theory Comput. 2019, 15, 2954−2965

Table 1. Singlet and Triplet Excitation Energies (unit: eV) of Five Types of Local Excitations of Noninteracting He Atoms as Shown in Figure 6[a]

				HP σ-SCF			
type	spin	FCI	U σ-SCF	He	He_2	He_3	He_4
(a)	T	40.02	45.76 (1.0)	40.02	40.02	40.02	40.02
	S	52.29		52.29	52.29	52.29	52.29
(b)	T	61.10	60.28 (1.0)	N/A	61.10	61.10	61.10
	S						
(c)	T_{T+T}	80.05	91.51 (2.0)	N/A	79.64	79.64	79.64
	S_{T+T}						
	T_{T+S}	92.31			91.90	91.90	91.90
	S_{S+S}	104.57			91.95	91.95	91.95
(d)	S	94.66	93.86 (0.0)	94.26	93.86	93.86	93.86
(e)	T	106.59	105.77 (1.0)	N/A	106.18	106.18	106.18
	S						

[a]For U σ-SCF states, $\langle \hat{S}^2 \rangle$ values are indicated in parentheses. The 6-31G basis is used for all calculations.

localized on m atoms and $n-m$ R σ-SCF ground states each localized on one atom, i.e.

$$|\Psi_n^{HP}\rangle = |\Psi_m^{HP}\rangle \otimes |\Psi_1^{R}\rangle^{\otimes(n-m)} \tag{27}$$

where $m = 1$ for a and 2 for b, c, and e, respectively. The HP σ-SCF ground state wave function has the same factorization as in eq 27 with $m = 1$. The size-intensivity of these excitations then follows naturally from the factorizations. For the local double excitation, d, the R σ-SCF solution remains stable under half-projection. Hence, for a single He atom, the difference between the unprojected and projected excitation energies arises solely from the HP correction to the ground state. This correction vanishes for $n \geq 2$ because it applies locally to one of the n He atoms in both the ground and excited state wave functions.

We note the reader that these results only suggest that local excitations in HP σ-SCF *can* be size-intensive if the corresponding wave functions are factorable as in eq 27. Here, the locality of the HP correction plays the key role. Indeed, for the selected excitations above, all delocalized HP σ-SCF states have higher variance compared to the localized ones. However, this may not hold in general, particularly for excitations that are delocalized over the whole molecule.

5. CONCLUSION

To summarize, we have applied the half-projection scheme to the recently developed excited state variational method, σ-SCF. The resulting theory, which we call HP σ-SCF, is not only as effective at locating electronic excitations as the original method but also exhibits substantial improvement on the quality of the broken-symmetry σ-SCF solutions through partially restoring the spin symmetry. Specifically, the benefits brought by half-projection are 2-fold. First, it recovers most static electron correlation for systems where spin-contamination from quintet (for singlet) and septet (for triplet) states is small and produces solutions whose PESs are in parallel with the exact solutions. Second, it largely suppresses the symmetry breaking-related unphysical behaviors of the unprojected σ-SCF solutions, such as disappearing solutions and discontinuous first-order energy derivatives. As a result, the HP σ-SCF PESs are smooth and extend over a wide range of geometries, which is key to postmean-field treatments such as NOCI. Furthermore, local excitations in HP σ-SCF can be size-intensive.

Despite all these advantages, HP σ-SCF can still fail under certain circumstances. First, as a two-determinant wave function method, HP σ-SCF is best at describing systems with only one or a few pairs of NOs exhibiting fractional occupation and, hence, fails when the exact state is truly multiconfigurational with a large number of fractionally occupied NOs. In those cases, the missing static correlation could potentially be recovered by a NOCI treatment using the HP σ-SCF solutions as quasi-diabatic bases, the effectiveness of which in turn relies on the smoothness and existence of the HP σ-SCF solutions as discussed above. Second, the dynamic part of the electron correlation is still missing in HP σ-SCF. Hence, it is insufficient for delivering quantitatively accurate excitation energies in a large basis.

In the future, HP σ-SCF could be extended in several directions. First, empirical observations suggest that more accurate and complete symmetry-projection could potentially lead to σ-SCF solutions that show less unphysical behaviors. The generator coordinate method,[105−107] which has been proven powerful in PQT,[38] is an ideal candidate for that purpose. Second, the dynamic correlation could be recovered in at least two different ways. On the one hand, wave function-based, many-body perturbation treatment using the mean-field excited state solutions as a starting point has already proven successful in the context of both single- and multireference (through NOCI) excited state solutions.[30,108−112] On the other hand, DFT also provides a computationally economic way to recover dynamic correlation; indeed, the Δ-SCF solutions to the Kohn−Sham equation have already proven successful as a complement to TDDFT.[22] The challenge of generalizing nonenergy-based mean-field methods (such as σ-SCF and its variants) to DFT is the lack of appropriate density functionals of relevant quantities in DFT that are key to those methods (e.g., energy variance for our purpose).

■ ASSOCIATED CONTENT

Supporting Information

The Supporting Information is available free of charge on the ACS Publications website at DOI: 10.1021/acs.jctc.8b01224.

(i) Expressions of the HP σ-SCF Fock matrices (sections S1 and S2), (ii) discussion on some general properties of HP wave functions (section S3), and (iii) unprojected σ-SCF solutions for H_2, LiH, and C_2H_4 as

DOI: 10.1021/acs.jctc.8b01224
J. Chem. Theory Comput. 2019, 15, 2954−2965

well as the NOCI solutions for H_2 (sections S4−S7) (PDF)

AUTHOR INFORMATION

Corresponding Author

*E-mail: tvan@mit.edu.

ORCID

Hong-Zhou Ye: 0000-0002-3714-2753

Troy Van Voorhis: 0000-0001-7111-0176

Notes

The authors declare no competing financial interest.

ACKNOWLEDGMENTS

H.-Z.Y. thanks Nathan Ricke for proofreading the manuscript. This work was funded by a grant from the NSF (Grant No. CHE-1464804). T.V.V. is a David and Lucille Packard Foundation Fellow.

REFERENCES

(1) Bene, J. E. D.; Ditchfield, R.; Pople, J. A. Self-Consistent Molecular Orbital Methods. X. Molecular Orbital Studies of Excited States with Minimal and Extended Basis Sets. *J. Chem. Phys.* **1971**, *55*, 2236−2241.

(2) Foresman, J. B.; Head-Gordon, M.; Pople, J. A.; Frisch, M. J. Toward a systematic molecular orbital theory for excited states. *J. Phys. Chem.* **1992**, *96*, 135−149.

(3) Runge, E.; Gross, E. K. U. Density-Functional Theory for Time-Dependent Systems. *Phys. Rev. Lett.* **1984**, *52*, 997−1000.

(4) Gross, E. K. U.; Kohn, W. Local density-functional theory of frequency-dependent linear response. *Phys. Rev. Lett.* **1985**, *55*, 2850−2852.

(5) Gross, E., Kohn, W. In *Density Functional Theory of Many-Fermion Systems*; Löwdin, P.-O., Ed.; Advances in Quantum Chemistry; Academic Press, 1990; Vol. *21*; pp 255−291.

(6) Casida, M. E. In *Recent Advances in Density Functional Methods (Part I)*; Chong, D. P., Ed.; Recent Advances in Computational Chemistry; World Scientific, 1995; Vol. *1*.

(7) Dreuw, A.; Head-Gordon, M. Single-Reference ab Initio Methods for the Calculation of Excited States of Large Molecules. *Chem. Rev.* **2005**, *105*, 4009−4037.

(8) Ziegler, T.; Krykunov, M. On the calculation of charge transfer transitions with standard density functionals using constrained variational density functional theory. *J. Chem. Phys.* **2010**, *133*, 074104.

(9) Krykunov, M.; Seth, M.; Ziegler, T. Introducing constricted variational density functional theory in its relaxed self-consistent formulation (RSCF-CV-DFT) as an alternative to adiabatic time dependent density functional theory for studies of charge transfer transitions. *J. Chem. Phys.* **2014**, *140*, 18A502.

(10) Tozer, D. J.; Handy, N. C. Improving virtual Kohn-Sham orbitals and eigenvalues: Application to excitation energies and static polarizabilities. *J. Chem. Phys.* **1998**, *109*, 10180−10189.

(11) Casida, M. E.; Salahub, D. R. Asymptotic correction approach to improving approximate exchange-correlation potentials: Time-dependent density-functional theory calculations of molecular excitation spectra. *J. Chem. Phys.* **2000**, *113*, 8918−8935.

(12) Tozer, D. J.; Handy, N. C. The importance of the asymptotic exchange-correlation potential in density functional theory. *Mol. Phys.* **2003**, *101*, 2669−2675.

(13) Dreuw, A.; Weisman, J. L.; Head-Gordon, M. Long-range charge-transfer excited states in time-dependent density functional theory require non-local exchange. *J. Chem. Phys.* **2003**, *119*, 2943−2946.

(14) Dreuw, A.; Head-Gordon, M. Failure of Time-Dependent Density Functional Theory for Long-Range Charge-Transfer Excited States: The Zincbacteriochlorin-Bacteriochlorin and Bacteriochlorophyll-Spheroidene Complexes. *J. Am. Chem. Soc.* **2004**, *126*, 4007−4016.

(15) Ziegler, T.; Seth, M.; Krykunov, M.; Autschbach, J.; Wang, F. On the relation between time-dependent and variational density functional theory approaches for the determination of excitation energies and transition moments. *J. Chem. Phys.* **2009**, *130*, 154102.

(16) Ziegler, T.; Krykunov, M.; Seidu, I.; Park, Y. C. *Density-Functional Methods for Excited States*; Top. Curr. Chem.; Springer, 2016; Vol. *368*; pp 61−95.

(17) Park, Y. C.; Senn, F.; Krykunov, M.; Ziegler, T. Self-Consistent Constricted Variational Theory RSCF-CV(ınfty)-DFT and Its Restrictions To Obtain a Numerically Stable ΔSCF-DFT-like Method: Theory and Calculations for Triplet States. *J. Chem. Theory Comput.* **2016**, *12*, 5438−5452.

(18) Hirata, S.; Head-Gordon, M. Time-dependent density functional theory within the Tamm-Dancoff approximation. *Chem. Phys. Lett.* **1999**, *314*, 291−299.

(19) Jones, R. O.; Gunnarsson, O. The density functional formalism, its applications and prospects. *Rev. Mod. Phys.* **1989**, *61*, 689−746.

(20) Hellman, A.; Razaznejad, B.; Lundqvist, B. I. Potential-energy surfaces for excited states in extended systems. *J. Chem. Phys.* **2004**, *120*, 4593−4602.

(21) Gavnholt, J.; Olsen, T.; Engelund, M.; Schiøtz, J. Δ self-consistent field method to obtain potential energy surfaces of excited molecules on surfaces. *Phys. Rev. B: Condens. Matter Mater. Phys.* **2008**, *78*, 075441.

(22) Gilbert, A. T. B.; Besley, N. A.; Gill, P. M. W. Self-Consistent Field Calculations of Excited States Using the Maximum Overlap Method (MOM). *J. Phys. Chem. A* **2008**, *112*, 13164−13171.

(23) Thom, A. J. W.; Head-Gordon, M. Locating Multiple Self-Consistent Field Solutions: An Approach Inspired by Metadynamics. *Phys. Rev. Lett.* **2008**, *101*, 193001.

(24) Thom, A. J. W.; Head-Gordon, M. Hartree-Fock solutions as a quasidiabatic basis for nonorthogonal configuration interaction. *J. Chem. Phys.* **2009**, *131*, 124113.

(25) Sundstrom, E. J.; Head-Gordon, M. Non-orthogonal configuration interaction for the calculation of multielectron excited states. *J. Chem. Phys.* **2014**, *140*, 114103.

(26) Malmqvist, P. A. Calculation of transition density matrices by nonunitary orbital transformations. *Int. J. Quantum Chem.* **1986**, *30*, 479−494.

(27) Zhao, L.; Neuscamman, E. An Efficient Variational Principle for the Direct Optimization of Excited States. *J. Chem. Theory Comput.* **2016**, *12*, 3436−3440.

(28) Ye, H.-Z.; Welborn, M.; Ricke, N. D.; Van Voorhis, T. σ-SCF: A direct energy-targeting method to mean-field excited states. *J. Chem. Phys.* **2017**, *147*, 214104.

(29) Shea, J. A. R.; Neuscamman, E. Size Consistent Excited States via Algorithmic Transformations between Variational Principles. *J. Chem. Theory Comput.* **2017**, *13*, 6078−6088.

(30) Shea, J. A. R.; Neuscamman, E. Communication: A mean field platform for excited state quantum chemistry. *J. Chem. Phys.* **2018**, *149*, 081101.

(31) Choi, J. H.; Lebeda, C. F.; Messmer, R. P. Variational principle for excited states: Exact formulation and other extensions. *Chem. Phys. Lett.* **1970**, *5*, 503−506.

(32) Bénard, M.; Paldus, J. Stability of Hartree-Fock solutions and symmetry breaking in the independent particle model: Ab initio case study of the LCAO-MO-SCF solutions for finite chains of hydrogen atoms. *J. Chem. Phys.* **1980**, *72*, 6546−6559.

(33) Paldus, J.; Čížek, J. Hartree-Fock stability and symmetry breaking: oxygen doubly negative ion. *Can. J. Chem.* **1985**, *63*, 1803−1811.

(34) Lepetit, M. B.; Malrieu, J. P.; Pelissier, M. Multiplicity of symmetry-broken Hartree-Fock solutions in multiple bonds and atomic clusters: An asymptotic view. *Phys. Rev. A: At., Mol., Opt. Phys.* **1989**, *39*, 981−991.

(35) Allen, W. D.; Horner, D. A.; Dekock, R. L.; Remington, R. B.; Schaefer, H. F. The lithium superoxide radical: Symmetry breaking

DOI: 10.1021/acs.jctc.8b01224
J. Chem. Theory Comput. 2019, 15, 2954−2965

phenomena and potential energy surfaces. *Chem. Phys.* **1989**, *133*, 11−45.
(36) Crawford, T. D.; Stanton, J. F.; Allen, W. D.; Schaefer, H. F. Hartree-Fock orbital instability envelopes in highly correlated single-reference wave functions. *J. Chem. Phys.* **1997**, *107*, 10626−10632.
(37) Mayer, I. In *The Spin-Projected Extended Hartree-Fock Method*; Löwdin, P.-O., Ed.; Advances in Quantum Chemistry; Academic Press, 1980; Vol. *12*; pp 189−262.
(38) Scuseria, G. E.; Jiménez-Hoyos, C. A.; Henderson, T. M.; Samanta, K.; Ellis, J. K. Projected quasiparticle theory for molecular electronic structure. *J. Chem. Phys.* **2011**, *135*, 124108.
(39) Jiménez-Hoyos, C. A.; Henderson, T. M.; Tsuchimochi, T.; Scuseria, G. E. Projected Hartree-Fock theory. *J. Chem. Phys.* **2012**, *136*, 164109.
(40) Löwdin, P.-O. Quantum Theory of Many-Particle Systems. III. Extension of the Hartree-Fock Scheme to Include Degenerate Systems and Correlation Effects. *Phys. Rev.* **1955**, *97*, 1509−1520.
(41) Lefebvre, R.; Dearman, H. H.; McConnell, H. M. Spin Densities in Odd Alternant Hydrocarbon Radicals. *J. Chem. Phys.* **1960**, *32*, 176−181.
(42) Lefebvre, R.; Smeyers, Y. G. Extended Hartree-Fock calculations for the helium ground state. *Int. J. Quantum Chem.* **1967**, *1*, 403−419.
(43) Lunell, S. Spin-Projected Hartree-Fock Calculations on the He-Like Ions Using General Spin Orbitals. *Phys. Rev. A: At., Mol., Opt. Phys.* **1970**, *1*, 360−369.
(44) Burden, F. R. An extended Hartree-Fock method using corresponding orbitals: Application to lithium hydride. *Int. J. Quantum Chem.* **1972**, *6*, 647−650.
(45) Rosenberg, M.; Martino, F. Spin projected extended Hartree-Fock calculations by direct minimization of the energy functional. *J. Chem. Phys.* **1975**, *63*, 5354−5361.
(46) Samanta, K.; Jiménez-Hoyos, C. A.; Scuseria, G. E. Exploring Copper Oxide Cores Using the Projected Hartree-Fock Method. *J. Chem. Theory Comput.* **2012**, *8*, 4944−4949.
(47) Rivero, P.; Jiménez-Hoyos, C. A.; Scuseria, G. E. Entanglement and Polyradical Character of Polycyclic Aromatic Hydrocarbons Predicted by Projected Hartree-Fock Theory. *J. Phys. Chem. B* **2013**, *117*, 12750−12758.
(48) Bytautas, L.; Jiménez-Hoyos, C. A.; Rodríguez-Guzmán, R.; Scuseria, G. E. Potential energy curves for Mo2: multi-component symmetry-projected Hartree-Fock and beyond. *Mol. Phys.* **2014**, *112*, 1938−1946.
(49) Rodríguez-Guzmán, R.; Jiménez-Hoyos, C. A.; Scuseria, G. E. Multireference symmetry-projected variational approximation for the ground state of the doped one-dimensional Hubbard model. *Phys. Rev. B: Condens. Matter Mater. Phys.* **2014**, *89*, 195109.
(50) Garza, A. J.; Jiménez-Hoyos, C. A.; Scuseria, G. E. Capturing static and dynamic correlations by a combination of projected Hartree-Fock and density functional theories. *J. Chem. Phys.* **2013**, *138*, 134102.
(51) Garza, A. J.; Jiménez-Hoyos, C. A.; Scuseria, G. E. Electronic correlation without double counting via a combination of spin projected Hartree-Fock and density functional theories. *J. Chem. Phys.* **2014**, *140*, 244102.
(52) Shi, H.; Jiménez-Hoyos, C. A.; Rodríguez-Guzmán, R.; Scuseria, G. E.; Zhang, S. Symmetry-projected wave functions in quantum Monte Carlo calculations. *Phys. Rev. B: Condens. Matter Mater. Phys.* **2014**, *89*, 125129.
(53) Amos, A. T.; Hall, G. G. Single determinant wave functions. *Proc. R. Soc. London A* **1961**, *263*, 483−493.
(54) Amos, A. T. Calculations on the ions and lowest π triplet states of some conjugated hydrocarbons. *Mol. Phys.* **1962**, *5*, 91−104.
(55) Amos, T.; Snyder, L. C. Unrestricted Hartree-Fock Calculations. I. An Improved Method of Computing Spin Properties. *J. Chem. Phys.* **1964**, *41*, 1773−1783.
(56) Snyder, L. C.; Amos, T. Unrestricted Hartree-Fock Calculations. II. Spin Properties of Pi-Electron Radicals. *J. Chem. Phys.* **1965**, *42*, 3670−3683.
(57) Hall, G. G., Amos, A. T. In *Molecular Orbital Theory of the Spin Properties of Conjugated Molecules*; Bates, D., Estermann, I., Eds.; Advances in Atomic and Molecular Physics; Academic Press, 1965; Vol. *1*; pp 1−59.
(58) Smeyers, Y. G.; Doreste-Suarez, L. Half-Projected and Projected Hartree-Fock Calculations for Singlet Ground States. I. four-Electron Atomic Systems. *Int. J. Quantum Chem.* **1973**, *7*, 687−698.
(59) Smeyers, Y. G.; Delgado-Barrio, G. Half-projected and projected Hartree-Fock calculations for singlet ground states. II. Lithium hydride. *Int. J. Quantum Chem.* **1974**, *8*, 733−743.
(60) Smeyers, Y. G.; Delgado-Barrio, G. Analysis of the half-projected Hartree-Fock function: Density matrix, natural orbitals, and configuration interaction equivalence. *Int. J. Quantum Chem.* **1976**, *10*, 461−472.
(61) Smeyers, Y. G.; Bruceñta, A. M. Half-projected Hartree-Fock model for computing potential-energy surfaces. *Int. J. Quantum Chem.* **1978**, *14*, 641−648.
(62) Cox, P. A.; Wood, M. H. The Half-Projected Hartree-Fock Method. I. Eigenvalue Formulation and Simple Applications. *Theoret. Chim. Acta* **1976**, *41*, 269−278.
(63) Cox, P. A.; Wood, M. H. The half-projected Hartree-Fock method. *Theoret. Chim. Acta* **1976**, *41*, 279−285.
(64) Szabo, A.; Ostlund, N. *Modern Quantum Chemistry: Introduction to Advanced Electronic Structure Theory*; Dover Books on Chemistry; Dover Publications, 1989.
(65) Rivero, P.; Jiménez-Hoyos, C. A.; Scuseria, G. E. Predicting Singlet-Triplet Energy Splittings with Projected Hartree-Fock Methods. *J. Phys. Chem. A* **2013**, *117*, 8073−8080.
(66) Hendeković, J.; Pavlović, M.; Sokolić, F. Generalization of Wick's theorem. *Chem. Phys. Lett.* **1981**, *77*, 382−386.
(67) Kong, L.; Nooijen, M.; Mukherjee, D. An algebraic proof of generalized Wick theorem. *J. Chem. Phys.* **2010**, *132*, 234107.
(68) Tsuchimochi, T.; Van Voorhis, T. Time-dependent projected Hartree-Fock. *J. Chem. Phys.* **2015**, *142*, 124103.
(69) Levy, B.; Berthier, G. Generalized brillouin theorem for multiconfigurational SCF theories. *Int. J. Quantum Chem.* **1968**, *2*, 307−319.
(70) Epstein, S. T., Ed. *The Variation Method in Quantum Chemistry*; Phys. Chem.; Elsevier, 1974; Vol. *33*; pp 57−68.
(71) Pian, J.; Sharma, C. S. The generalised Brillouin theorem. *J. Phys. A: Math. Gen.* **1981**, *14*, 1261.
(72) Chang, T. C.; Schwarz, W. H. E. Generalized brillouin theorem multiconfiguration method for excited states. *Theor. Chim. Acta* **1977**, *44*, 45−59.
(73) Pulay, P. Convergence acceleration of iterative sequences. the case of scf iteration. *Chem. Phys. Lett.* **1980**, *73*, 393−398.
(74) Weinstein, D. H. Modified Ritz Method. *Proc. Natl. Acad. Sci. U. S. A.* **1934**, *20*, 529−532.
(75) Hansen, E. R. Global optimization using interval analysis: The one-dimensional case. *J. Optim. Theory Appl.* **1979**, *29*, 331−344.
(76) Hellmann, H. *Einführung in die Quantenchemie*; Franz Deuticke, 1937.
(77) Feynman, R. P. Forces in Molecules. *Phys. Rev.* **1939**, *56*, 340−343.
(78) Ruedenberg, K.; Atchity, G. J. A quantum chemical determination of diabatic states. *J. Chem. Phys.* **1993**, *99*, 3799−3803.
(79) Atchity, G. J.; Ruedenberg, K. Determination of diabatic states through enforcement of configurational uniformity. *Theor. Chem. Acc.* **1997**, *97*, 47−58.
(80) Häser, M. Møller-Plesset (MP2) perturbation theory for large molecules. *Theor. Chim. Acta* **1993**, *87*, 147−173.
(81) Parrish, R. M.; Burns, L. A.; Smith, D. G. A.; Simmonett, A. C.; DePrince, A. E.; Hohenstein, E. G.; Bozkaya, U.; Sokolov, A. Y.; Di Remigio, R.; Richard, R. M.; Gonthier, J. F.; James, A. M.; McAlexander, H. R.; Kumar, A.; Saitow, M.; Wang, X.; Pritchard, B. P.; Verma, P.; Schaefer, H. F.; Patkowski, K.; King, R. A.; Valeev, E. F.; Evangelista, F. A.; Turney, J. M.; Crawford, T. D.; Sherrill, C. D. Psi4 1.1: An Open-Source Electronic Structure Program Emphasizing

DOI: 10.1021/acs.jctc.8b01224
J. Chem. Theory Comput. 2019, 15, 2954−2965

Automation, Advanced Libraries, and Interoperability. *J. Chem. Theory Comput.* **2017**, *13*, 3185−3197.
(82) Dunning, T. H. Gaussian basis sets for use in correlated molecular calculations. I. The atoms boron through neon and hydrogen. *J. Chem. Phys.* **1989**, *90*, 1007−1023.
(83) Shao, Y.; Gan, Z.; Epifanovsky, E.; Gilbert, A. T.; Wormit, M.; Kussmann, J.; Lange, A. W.; Behn, A.; Deng, J.; Feng, X.; Ghosh, D.; Goldey, M.; Horn, P. R.; Jacobson, L. D.; Kaliman, I.; Khaliullin, R. Z.; Kuś, T.; Landau, A.; Liu, J.; Proynov, E. I.; Rhee, Y. M.; Richard, R. M.; Rohrdanz, M. A.; Steele, R. P.; Sundstrom, E. J.; Woodcock, H., III; Zimmerman, P. M.; Zuev, D.; Albrecht, B.; Alguire, E.; Austin, B.; Beran, G. J. O.; Bernard, Y. A.; Berquist, E.; Brandhorst, K.; Bravaya, K. B.; Brown, S. T.; Casanova, D.; Chang, C.-M.; Chen, Y.; Chien, S. H.; Closser, K. D.; Crittenden, D. L.; Diedenhofen, M.; Distasio, R., Jr.; Do, H.; Dutoi, A. D.; Edgar, R. G.; Fatehi, S.; Fusti-Molnar, L.; Ghysels, A.; Golubeva-Zadorozhnaya, A.; Gomes, J.; Hanson-Heine, M. W.; Harbach, P. H.; Hauser, A. W.; Hohenstein, E. G.; Holden, Z. C.; Jagau, T.-C.; Ji, H.; Kaduk, B.; Khistyaev, K.; Kim, J.; Kim, J.; King, R. A.; Klunzinger, P.; Kosenkov, D.; Kowalczyk, T.; Krauter, C. M.; Lao, K. U.; Laurent, A. D.; Lawler, K. V.; Levchenko, S. V.; Lin, C. Y.; Liu, F.; Livshits, E.; Lochan, R. C.; Luenser, A.; Manohar, P.; Manzer, S. F.; Mao, S.-P.; Mardirossian, N.; Marenich, A. V.; Maurer, S. A.; Mayhall, N. J.; Neuscamman, E.; Oana, C. M.; Olivares-Amaya, R.; O'Neill, D. P.; Parkhill, J. A.; Perrine, T. M.; Peverati, R.; Prociuk, A.; Rehn, D. R.; Rosta, E.; Russ, N. J.; Sharada, S. M.; Sharma, S.; Small, D. W.; Sodt, A.; Stein, T.; Stück, D.; Su, Y.-C.; Thom, A. J.; Tsuchimochi, T.; Vanovschi, V.; Vogt, L.; Vydrov, O.; Wang, T.; Watson, M. A.; Wenzel, J.; White, A.; Williams, C. F.; Yang, J.; Yeganeh, S.; Yost, S. R.; You, Z.-Q.; Zhang, I. Y.; Zhang, X.; Zhao, Y.; Brooks, B. R.; Chan, G. K.; Chipman, D. M.; Cramer, C. J.; Goddard, W. A., III; Gordon, M. S.; Hehre, W. J.; Klamt, A.; Schaefer, H. F., III; Schmidt, M. W.; Sherrill, C. D.; Truhlar, D. G.; Warshel, A.; Xu, X.; Aspuru-Guzik, A.; Baer, R.; Bell, A. T.; Besley, N. A.; Chai, J.-D.; Dreuw, A.; Dunietz, B. D.; Furlani, T. R.; Gwaltney, S. R.; Hsu, C.-P.; Jung, Y.; Kong, J.; Lambrecht, D. S.; Liang, W.; Ochsenfeld, C.; Rassolov, V. A.; Slipchenko, L. V.; Subotnik, J. E.; Van Voorhis, T.; Herbert, J. M.; Krylov, A. I.; Gill, P. M.; Head-Gordon, M. Advances in molecular quantum chemistry contained in the Q-Chem 4 program package. *Mol. Phys.* **2015**, *113*, 184−215.
(84) Ye, H.-Z. Frankenstein: An Electronic Structure Method Development Platform. https://github.com/hongzhouye/frankenstein, 2018.
(85) White, S. R. Density matrix formulation for quantum renormalization groups. *Phys. Rev. Lett.* **1992**, *69*, 2863−2866.
(86) Verstraete, F.; Murg, V.; Cirac, J. I. Matrix product states, projected entangled pair states, and variational renormalization group methods for quantum spin systems. *Adv. Phys.* **2008**, *57*, 143−224.
(87) Chan, G. K.-L.; Head-Gordon, M. Highly correlated calculations with a polynomial cost algorithm: A study of the density matrix renormalization group. *J. Chem. Phys.* **2002**, *116*, 4462−4476.
(88) Chan, G. K.-L. An algorithm for large scale density matrix renormalization group calculations. *J. Chem. Phys.* **2004**, *120*, 3172−3178.
(89) Ghosh, D.; Hachmann, J.; Yanai, T.; Chan, G. K.-L. Orbital optimization in the density matrix renormalization group, with applications to polyenes and β-carotene. *J. Chem. Phys.* **2008**, *128*, 144117.
(90) Sharma, S.; Chan, G. K.-L. Spin-adapted density matrix renormalization group algorithms for quantum chemistry. *J. Chem. Phys.* **2012**, *136*, 124121.
(91) Olivares-Amaya, R.; Hu, W.; Nakatani, N.; Sharma, S.; Yang, J.; Chan, G. K.-L. The ab-initio density matrix renormalization group in practice. *J. Chem. Phys.* **2015**, *142*, 034102.
(92) Bouman, T. D.; Hansen, A. E.; Voigt, B.; Rettrup, S. Large-scale RPA calculations of chiroptical properties of organic molecules: Program RPAC. *Int. J. Quantum Chem.* **1983**, *23*, 595−611.
(93) Sun, Q.; Berkelbach, T. C.; Blunt, N. S.; Booth, G. H.; Guo, S.; Li, Z.; Liu, J.; McClain, J. D.; Sayfutyarova, E. R.; Sharma, S.; Wouters, S.; Chan, G. K.-L. PySCF: the Python-based simulations of chemistry framework. *WIREs Comput. Mol. Sci.* **2018**, *8*, e1340.
(94) Roos, B. O.; Taylor, P. R.; Siegbahn, P. E. M. A complete active space SCF method (CASSCF) using a density matrix formulated super-CI approach. *Chem. Phys.* **1980**, *48*, 157−173.
(95) Frisch, M. J.; Trucks, G. W.; Schlegel, H. B.; Scuseria, G. E.; Robb, M. A.; Cheeseman, J. R.; Montgomery, J. A., Jr.; Vreven, T.; Kudin, K. N.; Burant, J. C.; Millam, J. M.; Iyengar, S. S.; Tomasi, J.; Barone, V.; Mennucci, B.; Cossi, M.; Scalmani, G.; Rega, N.; Petersson, G. A.; Nakatsuji, H.; Hada, M.; Ehara, M.; Toyota, K.; Fukuda, R.; Hasegawa, J.; Ishida, M.; Nakajima, T.; Honda, Y.; Kitao, O.; Nakai, H.; Klene, M.; Li, X.; Knox, J. E.; Hratchian, H. P.; Cross, J. B.; Bakken, V.; Adamo, C.; Jaramillo, J.; Gomperts, R.; Stratmann, R. E.; Yazyev, O.; Austin, A. J.; Cammi, R.; Pomelli, C.; Ochterski, J. W.; Ayala, P. Y.; Morokuma, K.; Voth, G. A.; Salvador, P.; Dannenberg, J. J.; Zakrzewski, V. G.; Dapprich, S.; Daniels, A. D.; Strain, M. C.; Farkas, O.; Malick, D. K.; Rabuck, A. D.; Raghavachari, K.; Foresman, J. B.; Ortiz, J. V.; Cui, Q.; Baboul, A. G.; Clifford, S.; Cioslowski, J.; Stefanov, B. B.; Liu, G.; Liashenko, A.; Piskorz, P.; Komaromi, I.; Martin, R. L.; Fox, D. J.; Keith, T.; Al-Laham, M. A.; Peng, C. Y.; Nanayakkara, A.; Challacombe, M.; Gill, P. M. W.; Johnson, B.; Chen, W.; Wong, M. W.; Gonzalez, C.; Pople, J. A. *Gaussian 03*, Revision C.02; Gaussian, Inc., Wallingford, CT, 2004.
(96) Binkley, J. S.; Pople, J. A.; Hehre, W. J. Self-consistent molecular orbital methods. 21. Small split-valence basis sets for first-row elements. *J. Am. Chem. Soc.* **1980**, *102*, 939−947.
(97) Smeyers, Y. G. In *The half projected hartree-fock model for determining singlet excited states*; Löwdin, P.-O., Sabin, J. R., Zerner, M. C., Bmändas, E., Lami, A., Barone, V., Eds.; Adv. Quantum Chem.; Academic Press, 2000; Vol. *36*; pp 253−270.
(98) Hehre, W. J.; Stewart, R. F.; Pople, J. A. Self-Consistent Molecular-Orbital Methods. I. Use of Gaussian Expansions of Slater-Type Atomic Orbitals. *J. Chem. Phys.* **1969**, *51*, 2657−2664.
(99) We have tried increasing the number of states being averaged up to 16 as well as other software packages such as PySCF; neither removes the discontinuities of the SA-CASSCF solutions shown in Figure 5.
(100) Ukrainsky, I. I. Electronic structure of long cumulene chains. *Int. J. Quantum Chem.* **1972**, *6*, 473−489.
(101) Castaño, O.; Karadakov, P. The spin-unrestricted and the spin-projected HF methods: a comparison based on the stability properties of the closed-shell RHF solutions for large cyclic polyenes. *Chem. Phys. Lett.* **1986**, *130*, 123−126.
(102) Hirata, S. Thermodynamic limit and size-consistent design. *Theor. Chem. Acc.* **2011**, *129*, 727−746.
(103) Henderson, T. M.; Scuseria, G. E. Linearized Jastrow-style fluctuations on spin-projected Hartree-Fock. *J. Chem. Phys.* **2013**, *139*, 234113.
(104) Frisch, M. J.; Trucks, G. W.; Schlegel, H. B.; Scuseria, G. E.; Robb, M. A.; Cheeseman, J. R.; Scalmani, G.; Barone, V.; Mennucci, B.; Petersson, G. A.; Nakatsuji, H.; Caricato, M.; Li, X.; Hratchian, H. P.; Izmaylov, A. F.; Bloino, J.; Zheng, G.; Sonnenberg, J. L.; Hada, M.; Ehara, M.; Toyota, K.; Fukuda, R.; Hasegawa, J.; Ishida, M.; Nakajima, T.; Honda, Y.; Kitao, O.; Nakai, H.; Vreven, T.; Montgomery, J.; A, J.; Peralta, J. E.; Ogliaro, F.; Bearpark, M.; Heyd, J. J.; Brothers, E.; Kudin, K. N.; Staroverov, V. N.; Kobayashi, R.; Normand, J.; Raghavachari, K.; Rendell, A.; Burant, J. C.; Iyengar, S. S.; Tomasi, J.; Cossi, M.; Rega, N.; Millam, M. J.; Klene, M.; Knox, J. E.; Cross, J. B.; Bakken, V.; Adamo, C.; Jaramillo, J.; Gomperts, R.; Stratmann, R. E.; Yazyev, O.; Austin, A. J.; Cammi, R.; Pomelli, C.; Ochterski, J. W.; Martin, R. L.; Morokuma, K.; Zakrzewski, V. G.; Voth, G. A.; Salvador, P.; Dannenberg, J. J.; Dapprich, S.; Daniels, A. D.; Farkas, Ã.; Foresman, J. B.; Ortiz, J. V.; Cioslowski, J.; Fox, D. J. *Gaussian 09*, Revision E.01; Gaussian, Inc., Wallingford, CT, 2009.
(105) Tabakin, F. The generator coordinate method for nuclear scattering. *Nucl. Phys. A* **1972**, *182*, 497−521.
(106) Giraud, B. G.; Hahn, Y. Generator coordinate approach to nuclear reactions. I. Potential scattering of a nucleus and dynamical distortions. *Phys. Rev. C: Nucl. Phys.* **1981**, *23*, 1486−1494.

DOI: 10.1021/acs.jctc.8b01224
J. Chem. Theory Comput. 2019, 15, 2954−2965

(107) Hahn, Y.; Giraud, B. Generator coordinate approach to nuclear reactions. II. Nucleus-nucleus scattering with distorted basis functions. *Phys. Rev. C: Nucl. Phys.* **1981**, *23*, 1495−1502.
(108) Schlegel, H. B. Møller-Plesset perturbation theory with spin projection. *J. Phys. Chem.* **1988**, *92*, 3075−3078.
(109) Tsuchimochi, T.; Van Voorhis, T. Extended Møller-Plesset perturbation theory for dynamical and static correlations. *J. Chem. Phys.* **2014**, *141*, 164117.
(110) Yost, S. R.; Kowalczyk, T.; Van Voorhis, T. A multireference perturbation method using non-orthogonal Hartree-Fock determinants for ground and excited states. *J. Chem. Phys.* **2013**, *139*, 174104.
(111) Yost, S. R.; Head-Gordon, M. Size consistent formulations of the perturb-then-diagonalize Møller-Plesset perturbation theory correction to non-orthogonal configuration interaction. *J. Chem. Phys.* **2016**, *145*, 054105.
(112) Yost, S. R.; Head-Gordon, M. Efficient Implementation of NOCI-MP2 Using the Resolution of the Identity Approximation with Application to Charged Dimers and Long C-C Bonds in Ethane Derivatives. *J. Chem. Theory Comput.* **2018**, *14*, 4791−4805.

DOI: 10.1021/acs.jctc.8b01224
J. Chem. Theory Comput. 2019, 15, 2954−2965